Astronomical and Astrophysical Transactions (*AApTr*), 2017, Vol. 30, Issue 2, pp. 161–172,
ISSN 1055-6796, Photocopying permitted by license only, ©Cambridge Scientific Publishers

New results on Class I methanol masers in nearby low-mass star formation regions

S.V. Kalenskii[1,*], S. Kurtz[2], P. Hofner[3,4]

[1]*Astro Space Center, Lebedev Physical Institute, Profsoyuznaya 84/32, Moscow, 117997, Russia*
[2]*Instituto de Radioastronomia y Astrofizika, Universidad Nacional Autonoma de Mexico, Morelia, Michoacan, Mexico*
[3]*Physics Department, New Mexico Tech, 801 Leroy Place, Socorro, NM 87801, USA*
[4]*National Radio Astronomy Observatory, 1003 Lopezville Road, Socorro, NM 87801, USA*

Received 1 March, 2017

We present the review of the properties of Class I methanol masers detected in low-mass star forming regions (LMSFRs). These masers, called further LMMIs, are associated with postshock gas in the lobes of chemically active outflows in LMSFRs NGC1333, NGC2023, HH25, and L1157. Flux densities of these masers are no higher than 18 Jy at 44 GHz and are lower in the other Class I lines, being much lower than those of strong Class I masers in the regions of high-mass star formation. However, LMMI luminosities at 44 GHz match the relation "maser luminosity–protostar luminosity" established for high- and intermediate-mass protostars. No variability of LMMIs has been found in 2004–2011. Radial velocities of most LMMIs are close to the systemic velocities of associated regions. The only known exception is the maser detected at 36 GHz toward the blue lobe of the extra-high-velocity outflow in NGC2023, whose radial velocity is 3.5 km s^{-1} lower than the systemic velocity.

Four masers, NGC1333I2A, NGC1333I4A, HH25MMS, and L1157 have been observed at 44 GHz with the VLA in the D configuration with an angular resolution of about 1.5″. All of them except NGC1333I2A have been later reobserved with the EVLA in the B configuration, which provides an angular resolution of about 0.2″ at this frequency. The maser images consist of compact spots, unresolved or barely resolved even with the B configuration. The brightness temperatures of the strongest spots are hundreds of thousands Kelvins. Many spots consist of two spatial components and demonstrate double spectral lines.

An interesting result is the detection of unresolved spots demonstrating broad ($\gtrsim$3–5 km s^{-1}) spectral lines. Their fluxes correspond to brightness temperatures $\gtrsim$ 1000 K. Thus, in spite of large linewidths, these objects could be weak masers. Probably, the broad lines, detected in some sources at 44 GHz and in other Class I lines as a result of single-dish observations, are also masers.

We believe that turbulence plays an important role in forming the image and the spectrum of maser emission. However, turbulence alone cannot provide the observed

*Email: kalensky@asc.rssi.ru

intensities of masers in L1157. Therefore we believe that some additional factors are required in order to explain the observed LMMI properties.

Keywords: ISM: clouds: ISM: jets and outflows: ISM: molecules: masers: radio lines: ISM

1 Introduction

Bright and narrow maser lines of methanol (CH_3OH) have been found towards many star-forming regions (Haschick et al., 1990; Menten, 1991a; Kurtz et al., 2004). According to the classification of Menten (1991b), methanol masers can be divided into two classes, I and II, with each class characterized by a certain set of transitions. The Class I maser transitions are the $7_0 - 6_1A^+$ transition at 44 GHz, $4_{-1} - 3_0E$ transition at 36 GHz, $5_{-1} - 4_0E$ transition at 84 GHz, $6_{-1} - 5_0E$ transition at 132 GHz, $8_0 - 7_1A^+$ transition at 95 GHz etc., while the Class II transitions are the $5_1 - 6_0A^+$ transition at 6.7 GHz, $2_0 - 3_{-1}E$ transition at 12 GHz, the series of $J_0 - J_{-1}E$ transitions at 157 GHz, etc. The strongest methanol masers are Class II masers at 6.7 GHz, some of which achieve flux densities of ∼4000 Jy (Menten, 1991a). The strongest Class I masers emit at 44 GHz and demonstrate flux densities up to 800 Jy (Haschick et al., 1990). Class II masers, further called MMIIs, are located in close vicinities

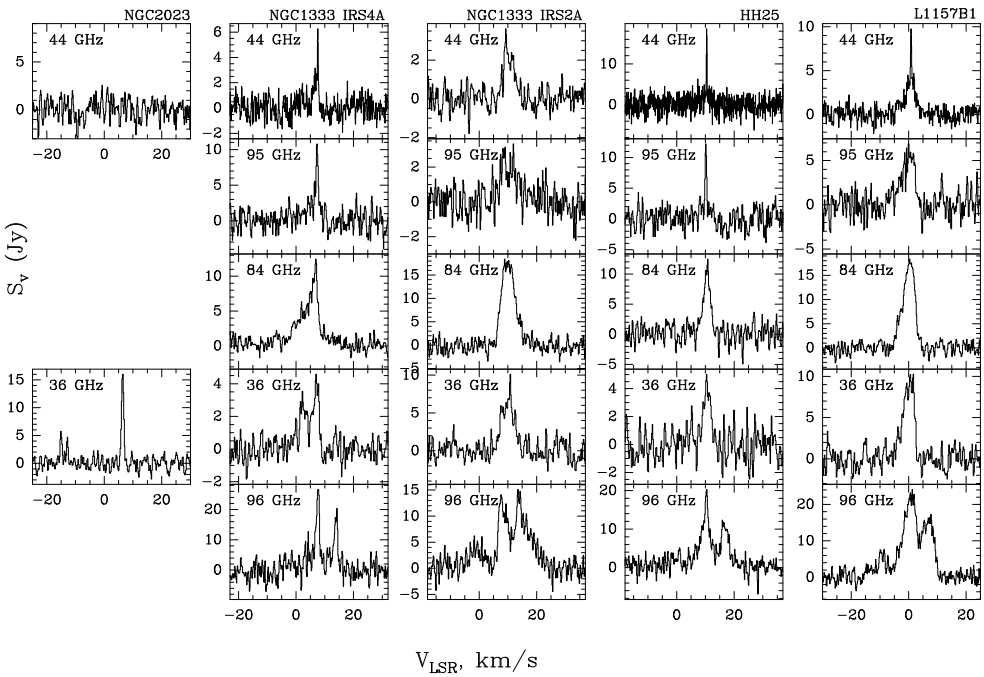


Figure 1 LMMI spectra in the $7_0 - 6_1A^+$ line at 44 GHz, the $8_0 - 7_1A^+$ line at 95 GHz, the $5_{-1} - 4_0E$ line at 84 GHz, and the $4_{-1} - 3_0E$ line at 36 GHz, taken at the Onsala Space Observatory. For comparison, purely thermal $2_K - 1_K$ methanol lines are shown in the bottom row.

of massive YSOs, while Class I masers (MMIs) are often seen offset of YSOs and are thought to be associated with shocks generated by bipolar outflows (Plambeck & Menten, 1990; Kurtz et al., 2004), supernova remnants (Pihlström et al., 2014), gas accretion (Kurtz et al., 2004), expanding HII regions (Voronkov et al., 2010), and cloud–cloud collisions (Sobolev et al., 1993). Only a very small number of Class I maser variations have been observed so far (e.g., Polushkin et al., 2009), while the variability of Class II masers is a much more common phenomenon, including periodic variability (Goedhart et al., 2012, and references therein).

Until recently it was considered that methanol masers arise only in massive star formation regions (MSFRs). But in the past few years several MMIs have been found in nearby low-mass star formation regions (LMSFRs) NGC1333, NGC2023, HH25, and L1157 (Kalenskii et al., 2006, 2010a; Kang et al., 2013; Lyo et al., 2014). The masers were detected in the Class I lines at 36 GHz, 44 GHz, 95 GHz, and 132 GHz. The study of Class I methanol masers in LMSFRs might be more straightforward compared to the study of the "classical" MMIs in MSFRs, because, in contrast to MSFRs, LMSFRs are widespread and many of them are located only 200–300 pc from the Sun; they are less heavily obscured in optical and IR wave ranges, and there are many isolated low-mass Young Stellar Objects (YSOs).

MMIs in LMSFRs (further called LMMIs) have been already studied for approximately ten years. In this paper we present the review of the current state of affairs in this field of research.

2 Observational results

2.1 Single-dish observations

As a result of several sets of observations between 2004–2008 with the 20-m Onsala radio telescope we detected LMMIs towards outflows powered by low-mass YSOs NGC1333I2A, NGC1333I4A, HH25MMS, and L1157mm in the $7_0 - 6_1 A^+$ transition at 44 GHz. One more maser was found in the $4_{-1} - 3_0 E$ line at 36 GHz towards the NGC2023 outflow; this maser has no counterpart at 44 GHz. Narrow lines, most likely of maser origin, were detected towards NGC1333I4A and HH25MMS in two other Class I lines, $5_{-1} - 4_0 E$ at 84 GHz and $8_0 - 7_1 A^+$ at 95 GHz. The spectra of the detected lines are shown in Fig. 1. Later Lyo et al. (2014) confirmed our results on the NGC1333 sources and found masers at 132 GHz towards NGC1333I2A, NGC1333I4A, and NGC1333IB.

Apart from narrow maser lines, broader (a few km s^{-1}) lines were detected toward several LMSFRs at 36, 44, 84, 95, and 132 GHz (Kalenskii et al., 2010a; Kang et al., 2013; Lyo et al., 2014). Since these lines are broad, they are usually considered as thermal. However, based on the ratios of intensities of different lines, Kalenskii et al. (2013) argued that the broad line in NGC1333I2A is a maser. Moreover, interferometric observations (Section 2.2) revealed several compact ($\lesssim 0.3''$) spots at 44 GHz that demonstrate broad lines. Therefore it is possible that the broad lines detected by Kalenskii et al. (2010a), Kang et al. (2013) and Lyo et al. (2014) are also masers.

It is known that within the range of densities and temperatures typical for molecular clouds in the Galaxy many Class I lines are inverted (Slysh et al., 1999). Therefore

the broad Class I lines with brightness temperatures typical for thermal lines that arise in extended clouds can, in principle, be treated as masers. However, such lines have no theoretical or observational distinctions between them and ordinary thermal lines and are usually treated as thermal or quasi-thermal, while the term "masers" is applied to compact bright spots, which usually, but not always, demonstrate narrow lines. We adhere to the second definition in this paper.

LMMI properties derived from single-dish data were studied by Kalenskii et al. (2010a, 2013). The results on LMMIs published later (Kang et al., 2013; Lyo et al., 2014) agree with the conclusions in these papers.

The main LMMI properties are as follows:

All known LMMIs are associated with chemically active bipolar outflows, where the abundance of methanol and many other molecules are enhanced due to grain mantles evaporation (Tafalla & Bachiller, 2011). The known LMMIs are associated with clouds where the column densities of methanol are no less than 10^{14} cm^{-2}. Kalenskii et al. (2010a) suggested that MMIs can arise only when methanol column density is above this value.

Flux densities of LMMIs are no higher than 18 Jy at 44 GHz and are lower in the other Class I lines (see Fig. 1). Thus, LMMI flux densities are much lower than those of strong HMMIs. However, according to Kalenskii et al. (2013), LMMI luminosities at 44 GHz match the relation "protostar luminosity–maser luminosity" $L_{\mathrm{CH_3OH}} = 1.71 \times 10^{-10} (L_{\mathrm{bol}})^{1.22}$, established for high- and intermediate-mass protostars by Bae et al. (2011).

A series of repeated observations of NGC1333I4A, HH25, and L1157 at 44 GHz, performed at Onsala in 2004–2011, did not show notable variability of these masers. Slight changes in the line shapes and intensities can be attributed to calibration uncertainties and poor signal-to-noise ratios.

Radial velocities of the most of LMMIs are close to the systemic velocities of associated regions. The only known exception is the maser detected at 36 GHz in NGC 2023, whose radial velocity is 3.5 km s^{-1} lower than the systemic velocity.

Thus, one can see that the main properties of LMMIs are similar to those of HMMIs. LMMIs are likely to be an extension of HMMI population toward low luminosities of both the masers and the associated YSOs.

2.2 Interferometric observations

2.2.1 Previous observations

First interferometric observations of LMMIs have been performed with the NRAO* VLA at 44 GHz in the D configuration (Kalenskii et al., 2010b, 2013). The source list consisted of NGC1333I2A, NGC1333I4A, HH25MMS, and L1157. Two spots were found in each source except NGC1333I4A. The brighter spot in each source was denoted M1, the weaker source, M2. The sizes of the brightest spots proved to be less than $1''$ and their brightness temperatures, no less than several thousand Kelvins. The parameters of individual spots are presented in Kalenskii et al. (2013).

*The National Radio Astronomy Observatory is operated by Associated Universities, Inc., under contract with the National Science Foundation

All the maser spots were detected towards outflow lobes. Thus, these observations confirm that methanol masers are related to bipolar outflows.

Both L1157M1 and L1157M2 spatially coincide with compact clumps B0a and B1a, respectively, previously detected as a result of interferometric observations with the PdB array (Benedettini et al., 2007) in thermal lines of methanol and some other molecules. These clumps are associated with the blue lobe of the L1157 bipolar outflow. Interestingly, in the methanol maps of Benedettini et al. (2007) the clump B0a, associated with M1, is much weaker than the clump B1a, associated with M2.

Both L1157M1 and L1157M2 show double lines at 44 GHz, which was interpreted as a signature of collapse in Kalenskii et al. (2010a). However, Kalenskii et al. (2013) noted that, if correct, such interpretation is specific for L1157, since no other observed maser exhibits a double line profile.

2.2.2 New observations

Spatial resolution of about $1.5''$, achievable at 44 GHz with the VLA in the D configuration, proved to be insufficient to resolve individual maser spots and measure their sizes and brightness temperatures. Therefore in 2013 we reobserved three LMMIs, HH25, NGC1333I4A, and L1157 at 44 GHz using EVLA in the B configuration, which provides an angular resolution about $0.2''$ at 44 GHz. Each source was to be observed in a narrow band with a 15.6 kHz spectral resolution (0.11 km s^{-1} at 44 GHz) and in parallel, in a wide band with a 2 MHz (13.6 km s^{-1}) resolution. Unfortunately, as a result of a correlator setup error L1157 was observed only with the 2-MHz resolution. Therefore for this source we have lost the radial velocity information, and the observed intensities of maser features are strongly affected by the dilution, i.e., they are reduced by factors ∼6–27, according to the widths of individual spectral features as determined by Kalenskii et al. (2010b).

We also concluded that the resolution of ≈5 arcsec achieved by Benedettini et al. (2007) in the observations of thermal methanol is too low to study the clumps in L1157, where methanol masers arise. Therefore we observed L1157 in the 5_K–4_K thermal lines of methanol at 241 GHz with the antenna array CARMA in the C configuration. This configuration provides an angular resolution of $\approx 1''$ at 241 GHz, which is by a factor of ∼5 higher than the resolution of Benedettini et al. (2007). Unfortunately we could perform only preliminary observations before CARMA was closed.

The full description of the EVLA and CARMA observations and data reduction will be given elsewhere (Kalenskii et al., 2017).

A collection of the overall maps of the three observed sources at 44 GHz and the maps of individual maser spots at the same frequency are shown in Figs. 2–4. For L1157, the positions of maser spots are drawn on the CARMA map of thermal emission in the $5_0 - 4_0A^+$ line at 241 GHz. The overall maps show that each source consists of several spots which appear as contiguous features. At the same time the maps of individual spots show that many of these can be decomposed into two unresolved compact subspots. In these cases the brightest subspot is denoted subspot a, the second brightest subspot, subspot b.

The weak halo, seen around the brightest spot in the "old" image of NGC1333I4A (i.e., in the image, obtained with the VLA in the D configuration; Fig. 3) proved to

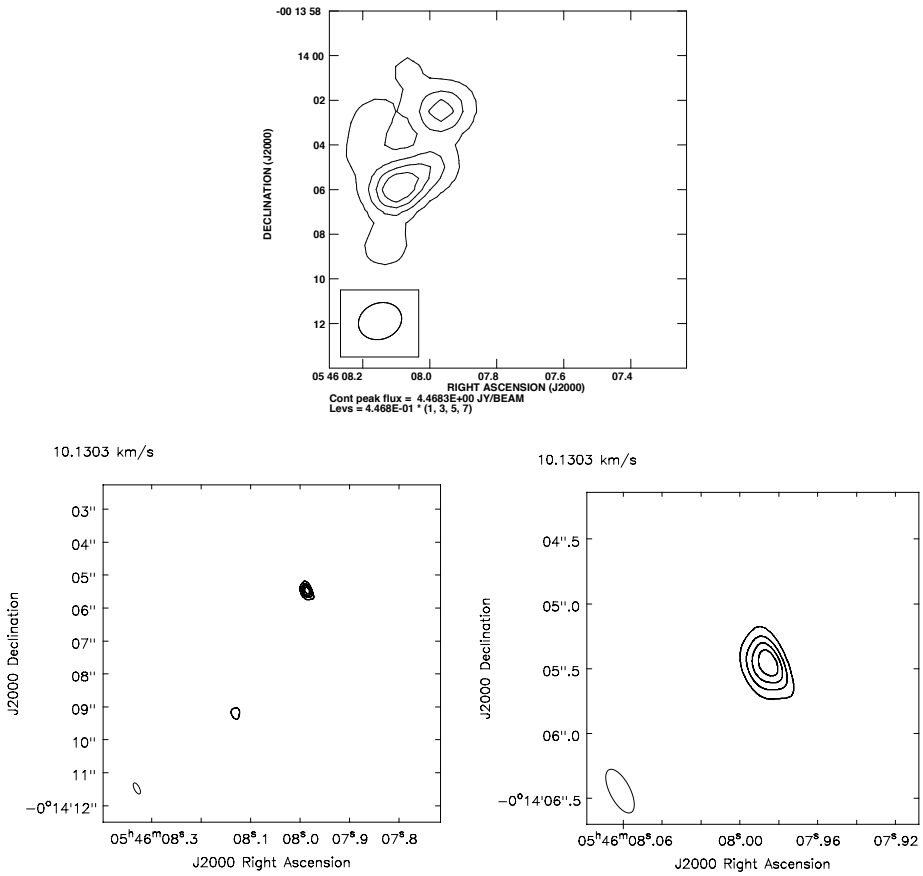


Figure 2 Masers in HH25, observed at 44 GHz with an angular resolution of 1.5″ (upper) and 0.2″ (lower left). Lower right: the strongest spot at a 0.2″ resolution.

consist of compact spots. The spots form an arc, suggesting a bow shock. However, there is no suitable known YSO that may drive an outflow responsible for such shock. A possible explanation is that the shock origin is e.g. the collision of two very compact clumps, similar to those detected by Benedettini et al. (2007) in L1157.

The old and new images of HH25 (i.e., obtained in the D and B configurations, respectively) are very different (see Fig. 2). On the one hand, this fact might point on a significant variation of this source between 2010 and 2013. We think, however, that a more plausible explanation of these differences is the existence of clumps with sizes 1″–2″ and moderate surface brightnesses, which can be seen as the strongest features in the old maps but are completely resolved in the new maps.

Some spots or subspots are unresolved or barely resolved in the new maps with a ∼0.2″ angular resolution. Thus, higher resolution is necessary to image them. The brightest of these demonstrate narrow spectral features and have brightness temperatures higher than 100000 K. For example, the size of the brightest clump in HH25, convolved with the beam, are $0.38'' \times 0.23''$. The measured flux of ∼8 Jy corresponds

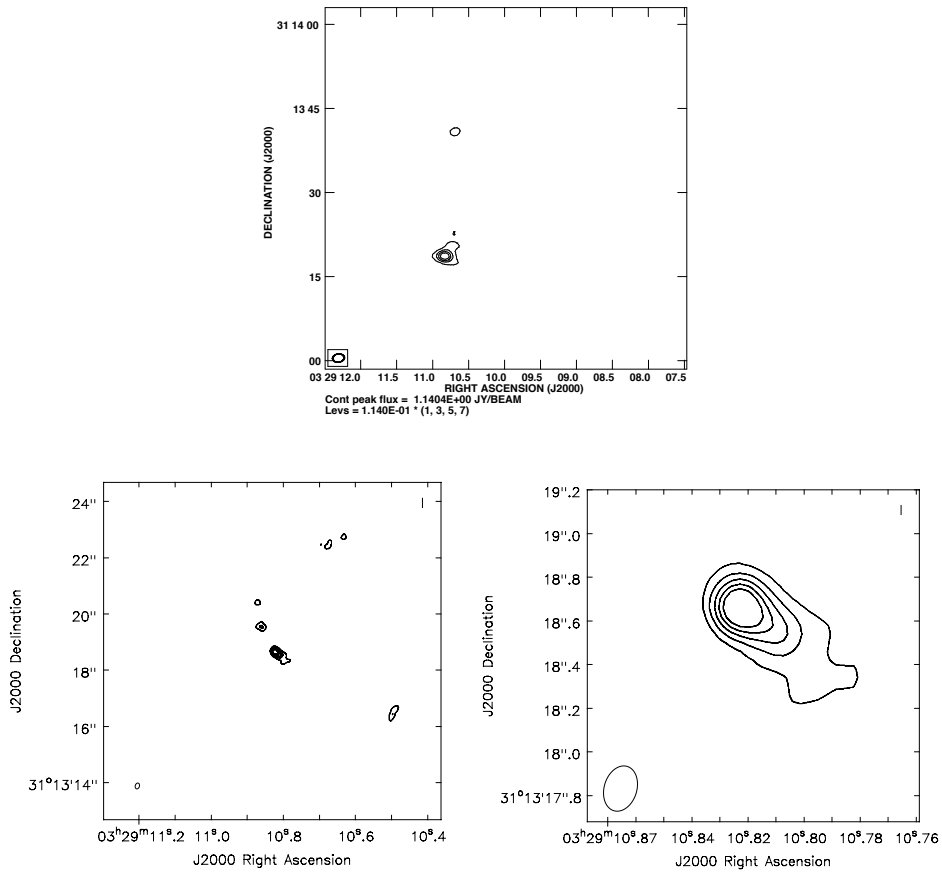


Figure 3 Masers at 44 GHz in NGC1333I4a with an angular resolution of 1.5″ (upper) and 0.2″ (lower left). Lower right: the strongest spot with a 0.2″ resolution.

to a brightness temperature of ∼60000 K. The sizes of this spot deconvolved from the beam are 0.16″ × 0.07″, yielding a brightness temperature of ∼500000 K.

Among the spots that demonstrate double structures are L1157M1 and M2, NGC1333I4A M2, etc†. There are several double spots where the spot components are so closely spaced that it is difficult to distinguish them in the overall source maps. An example of such double spot is shown in Fig. 5, which exhibits the channel map of the second brightest spot in HH25 (HH25M2). The image in the channel corresponding to $V_{lsr} = 10.024$ km s^{-1} consists of two spots shifted with respect to each other in the NW–SE direction by ∼0.15″. The images in other channels consist of single spots, with the higher-velocity spots coinciding with the SE spot, and the lower-velocity spots, with the NW spot.

An interesting result is the detection of unresolved spots demonstrating broad ($\gtrsim$3–5 km s^{-1}) spectral lines. Their fluxes are about 0.1–0.2 Jy/K, which corresponds

†Hereinafter M1 means the strongest spot in the new maps, M2 is the second strongest spot in the new maps etc.

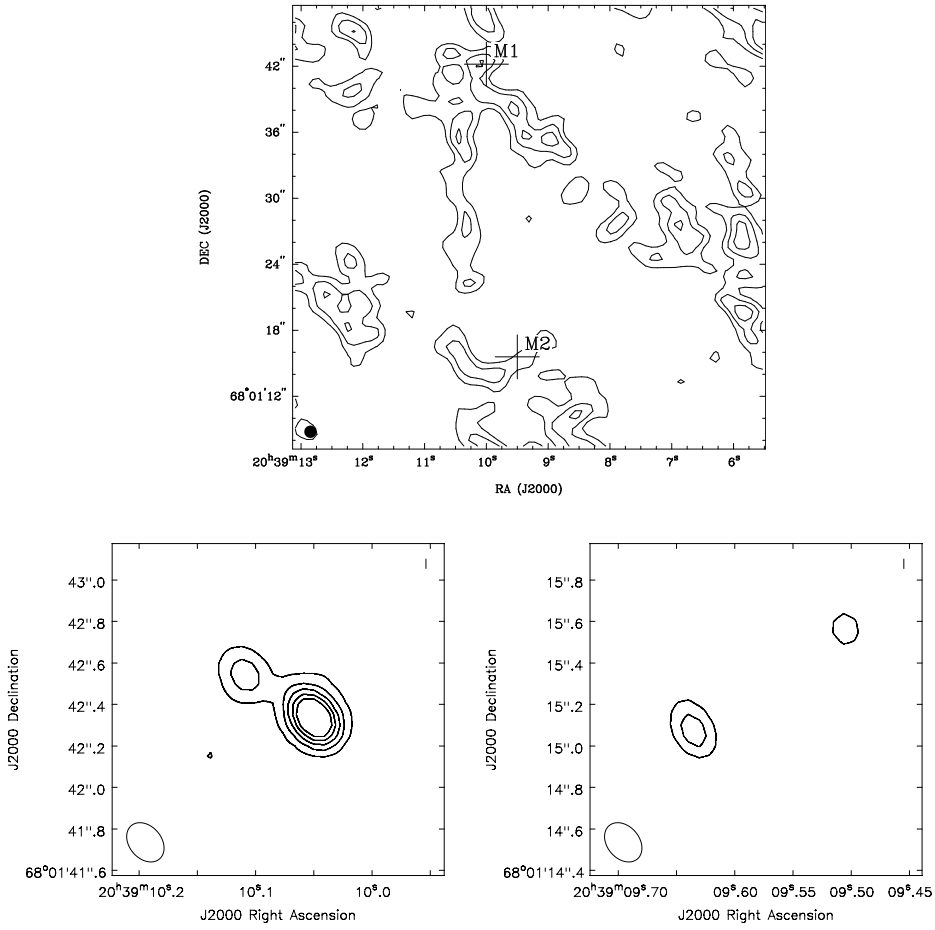


Figure 4 Upper panel: masers at 44 GHz (crosses) in L1157 overlaid upon the map of thermal methanol emission at 241 GHz. Lower left panel: the stronger spot (M1) at a 0.2″ resolution. Lower right panel: the weaker spot (M2) at a 0.2″ resolution.

to brightness temperatures $\gtrsim$1000 K. Thus, in spite of large linewidths, these objects are probably weak masers. Probably, the broad lines, detected at 44 GHz and in other Class I lines as a result of single-dish observations (see Section 2.1) are also masers.

3 Maser models

It is well known that the radial velocities of methanol masers are very close to the systemic velocities of the regions that host the masers. The differences between the maser and systemic velocities are usually no larger than 2–3 km s^{-1}, so that the radial velocities of methanol masers are located within the profiles of thermal lines in the relevant regions. Therefore in spite of the fact that methanol can belong to the jet

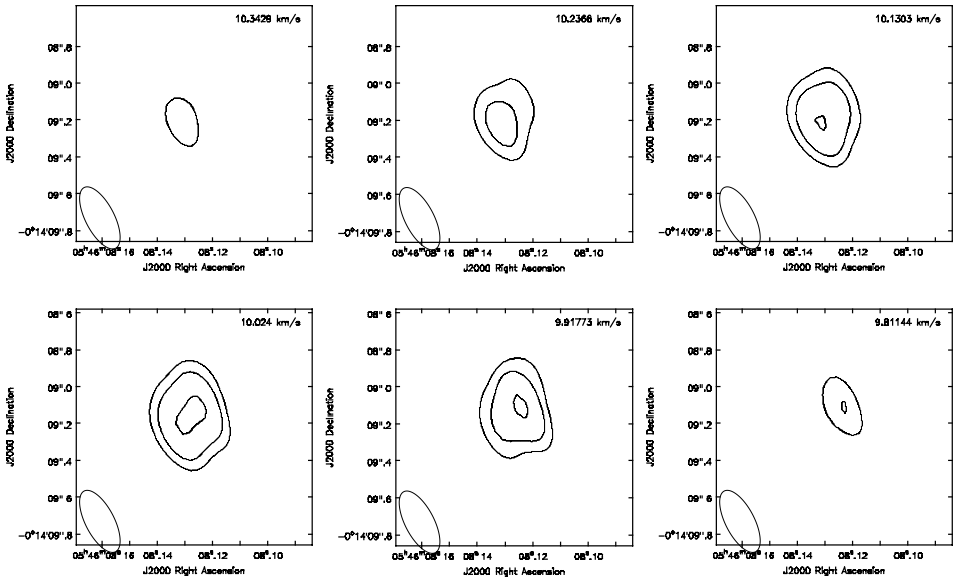


Figure 5 Channel maps of the M2 spot in HH25.

material (Tafalla & Bachiller, 2011) methanol masers most likely arise in postshock ambient gas.

All the known LMMIs are associated with outflows whose axes are located nearly perpendicular to the line of sight. One the one hand, this makes the aforementioned conclusion doubtful in the case of LMMIs. On the other hand, just in so oriented outflows we can check this conclusion observationally by measuring the maser proper motions. Assuming a fairly moderate projected flow velocity of 30 km s^{-1} and a source distance 300 pc we obtain a proper motion of $0.02''$ per year. Thus, if the masers are associated with high-velocity jets their positions will shift by about $0.2''$ during a time interval of 10 years. Such shifts of sufficiently compact sources can be measured with the VLA.

During the last decades the point of view that compact maser spots arise in much more extended clouds due to more suitable conditions for maser amplification along some lines inside the cloud became prevailing. The fact that methanol masers can arise only in the clouds with sufficiently high column density of methanol also agrees with this viewpoint. Sobolev et al. (1998) considered a model, which predicts that compact maser spots arise in extended turbulent clumps because in a turbulent velocity field the coherence lengths l along some lines are increased. In the case of unsaturated masers the maser intensity is proportional to $\exp(l)$, leading to the appearance of bright spots toward these directions.

Applicability of the model of Sobolev et al. (1998) to the masers in L1157 was examined by Kalenskii et al. (2010b). One of the main parameters of this model is τ_0, the absolute value of the optical depth at the center of the inverted line when there is no turbulence in the cloud. This value can be estimated provided that the column density of methanol N_{CH_3OH} is known. Benedettini et al. (2007) obtained $N_{CH_3OH} \sim$

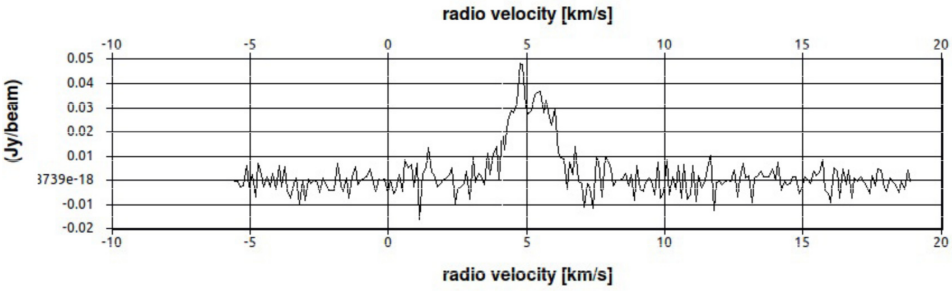


Figure 6 Spectra of the M2 spot in NGC1333I4A.

10^{16} cm^{-2} toward the clump B0a, which hosts the strongest methanol maser in this region from the intensity of the $2_0 - 1_0A^+$ line; approximately the same value can be derived from the intensity of the $5_0 - 4_0A^+$ line in our map (Fig. 4). Kalenskii et al. (2010b) showed that for this $N_{\mathrm{CH_3OH}}$ value the upper limit on τ_0 in clump B0a is about 10. Such optical depth makes it possible to explain the observed maser brightnesses. However, according to Table 1 of Sobolev et al. (1998) the maximum absolute values of optical depths *in the presence of turbulence* τ_{turb} are twice or more lower than the relevant τ_0 values. In addition, the column density of methanol determined from a single line integrated intencity may be highly erroneous; when the line's energy levels belong to the backbone ladder, as in the case of the $2_0 - 1_0A^+$ and $5_0 - 4_0A^+$ lines, the obtained column density is likely to be overestimated (Kalenskii et al., 2016). Therefore we believe that τ_0 in B0a is about 3–5 and τ_{turb} is even smaller. Such optical depth can produce a maser amplification of ∼15–20, which is clearly insufficient to explain the observed maser brightnesses.

Thus, although we are sure that turbulence plays an important role in forming maser images it seems unlikely that the masers in L1157 arises *merely* as a result of turbulence in the clumps that harbor the masers. Another fact, that in our opinion can be hardly explained within the frames of a purely turbulent model is a fairly high fraction of just double spots. The velocities of individual spots in such double structures are also different (Figs. 5, 6). This picture is traditionally explained in terms of rotating disk- or ring-like structures. A single turbulent eddie can in principle provide such double structure, but it is unclear why some individual eddies may be distinguished.

4 Summary

Several Class I methanol masers have been detected in three regions of low-mass star formation, NGC1333, HH25, and L1157. All these masers are associated with post-shock gas in the lobes of chemically active outflows, where the abundances of methanol and some other molecules are enhanced up to several orders of magnitude. The column densities of methanol toward the detected masers are no less than $\sim 10^{14}$ cm^{-2}. Flux densities of LMMIs are no higher than 18 Jy at 44 GHz and are lower in the other Class I lines, being much lower than those of strong HMMIs. However, LMMI luminosities at 44 GHz match the relation "maser luminosity–protostar luminosity"

established for high- and intermediate-mass protostars. No variability of LMMIs have been found in 2004–2011. Radial velocities of the most of LMMIs are close to the systemic velocities of associated regions.The only known exception is the maser detected at 36 GHz towards the blue lobe of the extra-high-velocity outflow in NGC 2023, whose radial velocity is 3.5 km s^{-1} lower than the systemic velocity.

Four masers, NGC1333I2A, NGC1333I4A, HH25MMS, and L1157 have been observed at 44 GHz with the VLA in the D configuration with an angular resolution of about 1.5″. All of them except NGC1333I2A have been reobserved with the EVLA in the B configuration, which provides an angular resolution of about 0.2″ at 44 GHz. The maser images consist of compact spots, unresolved or barely resolved even with the B configuration. The brightness temperatures of the strongest spots are hundreds of thousands Kelvins. Some spots consist of two spatial components and demonstrate double spectral lines.

The arc of maser spots in NGC1333I4A suggests a bow shock. However, there is no known protostellar object that could be responsible for this shock.

The images of HH25, obtained with the VLA in the D and B configurations, are very different. This fact might point to variability of this source between 2010 and 2013. However, a more plausible explanation of the differences between the images is the existence of clumps with sizes 1″–2″ and low brightnesses, which are seen as the strongest features in the lower resolution maps but proved to be completely resolved in the new maps.

An interesting result is the detection of unresolved spots demonstrating broad ($\gtrsim$3–5 km s^{-1}) spectral lines. Their fluxes correspond to brightness temperatures $\gtrsim$1000 K. Thus, in spite of large linewidths, these objects should be weak masers. Probably, the broad lines, detected in some sources at 44 GHz and in other Class I lines as a result of single-dish observations are also masers.

We believe that turbulence plays an important role in forming the image and the spectrum of maser emission. However, turbulence alone cannot explain the observed intensities of masers in L1157. Some kind of inhomogeneity of the clumps that harbor these masers is required.

Acknowledgments The authors are grateful to the OSO and VLA staffs who made it possible to perform the observations. The work was partially supported by the Russian Foundation for Basic Research (grants no. 10-02-00147 and 15-02-07676). PH acknowledges partial support from NSF grant AST-0908901. The Onsala Space Observatory is the Swedish National Facility for Radio Astronomy and is operated by Chalmers University of Technology, Göteborg, Sweden, with financial support from the Swedish Research Council and the Swedish Board for Technical Development.

References

Bachiller R., Perez Gutierrez M., Kumar M.S.N., Tafalla M., 2001, A&A, 372, 899

Bae J.-H., Kim, K.-T., Youn S.-Y., Kim W.-J., Byun D.-Y., Kang H., Oh C.S., 2011, ApJS, 196, 21

Benedettini M., Viti S., Codella C., Bachiller R., Gueth F., Beltran M.T., Dutrey A., Guilloteau S., 2007, Mon. Not. R. Astron. Soc., 381, 1127

Cragg D.M., Johns K.P., Godfrey P.D., Brown R.D., 1992, Mon. Not. R. Astron. Soc., 259, 203
Haschick A.D., Menten K.M., Baan W., 1990, ApJ, 354, 556
Goedhart S., Gaylard M., van der Walt J. in: *Cosmic masers: from OH to H0,* Ed. by R.S. Booth, E.M.L. Humphreys, and W.T.H. Vlemmings (Cambridge Univ. Press, 2012), p. 85
Kalenskii S.V., Promyslov V.G., Slysh V.I., Bergman P., Winnberg A., 2006, Astronomy Reports, 50, 289
Kalenskii S.V., Johansson L.E.B., Bergman P., Kurtz S., Hofner P., Walmsley C.M., Slysh V.I., 2010a, Mon. Not. R. Astron. Soc., 405, 613
Kalenskii S.V., Kurtz S., Slysh V.I., Hofner P., Walmsley C.M., Johansson L.E.B., Bergman P., 2010b, Astronomy Reports, 54, 932
Kalenskii S.V., Kurtz S., Bergman P., 2013, Astronomy Reports, 57, 120
Kalenskii S.V., Kurtz S., 2016, Astronomy Reports, 60, 702
Kalenskii S.V., Kurtz S., Hofner P., 2018, in preparation
Kang M., Lee J.-E., Choi M., Choi Y., Kim K.-T., Di Francesco J., Park Y.-S., 2013, ApJS, 209, 25
Kurtz S., Hofner P., Alvarez C.V., 2004, ApJS, 155, 149
Lyo, A.-R., Kim, J., Byun, D.-Y., Lee, H.-G., 2014, AJ 148, 80
Menten K.M., 1991a, ApJ, 380, L75
Menten K.M., 1991b, in Haschick A.D., Ho P.T.P., eds, Proc. 3rd Haystack Observatory Meeting, Skylines, Astron. Soc. Pac. Conf. Ser., 16, 119
Menten K.M., Walmsley C.M., Henkel C., Wilson T.L., 1988, A&A, 198, 253
Pihlström Y.M., Sjouwerman L.O., Frail D.A., Claussen M.J., Mesler R.A., McEwen B.C., 2014, AJ, 147, 73
Plambeck R.L., Menten K.M., 1990, ApJ, 364, 555
Polushkin S.V., Val'tts I.E., Slysh V.I., 2009, Astron. Rep., 53, 113
Slysh V.I., Kalenskii S.V., Val'tts I.E., Golubev V., 1999, ApJS, 123, 515
Sobolev A.M., 1993, Lect. Notes Phys., 412, 219
Sobolev A.M., Wallin B.K., Watson W.D., 1998, ApJ, 498, 763
Tafalla M. & Bachiller R., 2011, The Molecular Universe, *Proc. IAU Symp. 280,* J. Cernicharo and R. Bachiller, eds, p. 88
Voronkov M.A., Caswell J.L., Britton T.R., Green J.A., Sobolev A.M., Ellingsen S.P., 2010, Mon. Not. R. Astron. Soc., 408, 133